DISSERTATION

COLORADO STATE UNIV'S THESIS TEMPLATE

Submitted by

Matthew Gregory Hogan

Department of Physics

In partial fulfillment of the requirements

For the Degree of Doctor of Philosophy

Colorado State University

Fort Collins, Colorado

Summer 2019

Doctoral Committee:

Advisor: Walter Toki
Co-Advisor: Robert Wilson

Norman Buchanan
Wen Zhou

ABSTRACT

COLORADO STATE UNIV'S THESIS TEMPLATE

This document aims to get you started typesetting your thesis or dissertation in LaTeX.

ACKNOWLEDGEMENTS

I would like to thank the Elliott Forney for making a publicly accessible LaTeX template

TABLE OF CONTENTS

LIST OF TABLES

LIST OF FIGURES

Chapter 1

Introduction

Chose trop vue n'est chère tenue

A thing too much seen is little prized

French proverb

This describes the thesis

1.1 Introduction to Neutrinos

The history of the neutrino can be traced back to electron energy spectrum observed in neutron β-decay. While measurements of α- and γ-decay of atomic nuclei showed discrete spectral lines, the electron (β particle) exhibited a continuous energy spectrum. Experimentally, there were two observed particles in each decay process and classical physics dictated that the outgoing daughter particles should have discrete energies. The fact that the β-decay spectrum was not this way posed a fundamental problem for physicists in the mid-1910s and later, was energy conserved? Two solutions were postulated: either the "energy conservation law is only valid statistically in such a process [...] or an additional undetectable new particle [...] carrying away the additional energy and spin [...] is emitted [21]." The latter solution was supported by Wolfgang Pauli in a letter dated 4 December 1930 to a group of physicists meeting in Tübingen, modern Germany, where he first proposed what we would call a neutrino today[1]. Pauli's solution also predicted that the undetected neutrino would have half-integer spin, a quantum mechanical property of matter, since the observed particles in β-decay did not conserve angular momentum. The existence of the neutrino and validation of Pauli's predictions would not experimentally verified for another 20 years.

The neutrino was first discovered in 1953 by Clyde Cowan and Frederick Reines using a nuclear reactor in South Carolina, U.S.A.. Since then three types of neutrinos have been observed and from unique sources like the Sun and a supernova. Neutrino physics continues to be an active region of physics since neutrinos are unique probes to processes otherwise inaccessible in laboratories. For instance in the depths of the Sun's core where fusion occurs

[1] In W Pauli's December 1930 letter, he referred to his proposed particle as the "neutron", which is not the same neutron we know of today. At that point in time, the neutral particles inside the atomic nucleus, also called "neutrons", had not been discovered, let alone understood. The neutron, which was discovered in 1932 by James Chadwick, has been formally associated as the neutral, cousin particle to the proton. It would be Enrico Fermi who would coin the particle in W Pauli's letter and solution to the β-decay spectrum a "neutrino", meaning *little neutral one*.

and neutrinos are created, neutrinos are able to travel through the ultra dense and hot medium of the core (over 10^7 degrees Kelvin) and outer layers of the Sun and reach us on Earth.

Neutrinos rarely interact with normal matter, meaning that they travel essentially unimpeded towards one's particle detector. The rarity of such interactions can be illustrated with the fact that given nearly 7.0×10^{10} neutrinos/cm^2/sec^2 are incident on the Earth from the Sun, statistically one solar neutrino can harmlessly interact with an individual. So this begs the question: how does one detect a neutrino? The short answer is one needs a ultra large volume of matter and a large enough flux of neutrinos in its path just to detect one given today's technology.

Scientists continue to be interested in neutrinos due to properties they exhibit. One of the more recent and surprising aspects about neutrinos is their ability to undergo "flavor oscillations" where a neutrino of definite flavor (type) is created and later observed as a different flavor. The impact of such oscillations could help explain the observed matter and anti-matter asymmetry in the Universe.

1.1.1 Neutrinos in the Standard Model

The Standard Model (SM) of particle physics is the theory that describes the electromagnetic, strong nuclear, and weak nuclear forces and the elementary particles therein. These three forces and the gravitational force constitute the four *known* fundamental forces of the Universe. Each force in the SM has at least one "force carrier" particle that mediates the interactions between particles. The force carriers are formally called "gauge bosons" which indicates they are particles with integer $(0, 1, 2, ...)$ spin that come in temporary but unobservable existence to mediate the interaction. The weak nuclear bosons, the charged $W^{\pm}$ and neutral Z, couple to neutrinos as well as the other fermions, particles with half-integer

[2] To give some perspective to this number, this means 70 billion neutrinos are travelling every second through an area similar to one's own thumb nail.

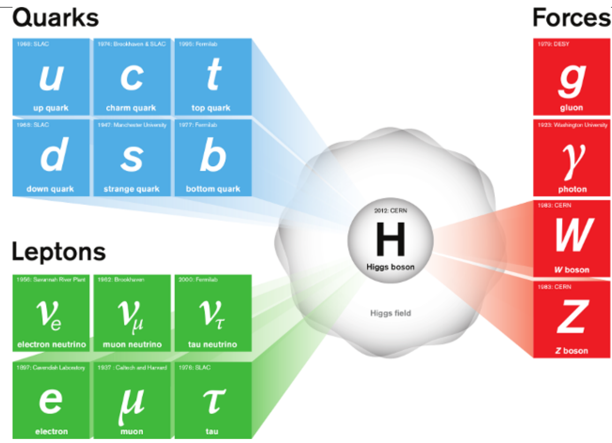

Figure 1.1: The Standard Model of particle physics consists of six quarks (up, down, strange, charm, bottom, and top), six leptons (electron, muon, tau, electron neutrino, muon neutrino, and tau neutrino), four force propagating bosons (gluon, photon, W, and Z), and the Higgs boson. The quarks, electron, muon, tau, W, and Z all gain mass through the Higgs field. The focus of this thesis are the neutrinos which are classified according to their charged, more massive Lepton cousins. Image taken from [4].

$\left(\frac{1}{2}, \frac{3}{2}, \frac{5}{2}, \ldots\right)$ spin, in the SM. All the elementary particles of the SM are shown in Figure 1.1 on page 4 .

Neutrinos in the SM are electrically neutral, massless particles categorized into three generations based on their charged, more massive Lepton cousins. The neutrino and charged lepton pair into a "weak isospin doublet" in the SM. These doublets are locally gauge invariant under a SU(2)$\times$U(1) symmetry which leads to the required existence of the photon and W and Z bosons[3].

What follows is a brief introduction to neutrino interactions as well as some of their fundamental properties.

[3] A gauge theory describes ways to measure physical forces or fields through interactions between elementary particles. The electric or magnetic fields for example can only be probed by charged particles. In the realm of quantum field theories, fields are postulated to permeate everywhere and it is excitations of these fields which produce experimental observables. Fields are constructed using the Lagrangian formalism and altered using gauge transformations. If altering the Lagrangian in some way does not affect the observables, this is referred to as a gauge invariance. Local gauge invariance means that under the constraints of the experiment, certain gauge transformations do not affect the observables. The allowed locally gauge invariant transformations require knowledge of its underlying Lie, or symmetry, group. With the weak isospin doublets, the Lie groups are SU(2)$\times$U(1) where SU(2) is the special unitary group of 2x2 unitary matrices, and U(1) is the unitary (circle) group consisting of complex numbers of magnitude 1.

1.1.1.1 Neutrino Weak Interactions

The name "weak force" comes from the fact that this force is has a much smaller effective range than the electromagnetic, strong nuclear, and gravitational forces. This is due to the weak mediating bosons, the $W^{\pm}$ and Z, being massive particles unlike the massless gluon (g) and photon (γ). The W/Z have masses of 80/90 GeV/c^2, which is more massive than all the elementary particles except for the top quark. For weak interactions to occur at energies far below the masses (also called "off-shell") of the W and Z, the interaction time must be infinitesimally small as dictated by the Heisenberg Uncertainty Principle

$$\Delta E \Delta t \gtrsim \hbar \tag{1.1}$$

where ΔE is the energy of the particle and Δt is the time which the particle exists.

Weak interactions are classified into two classes: charged current (CC) and neutral current (NC). CC interactions involve one of the two charged W bosons and change the incoming neutrino of flavor ν_l ($l = e, \mu, \tau$) into a electrically charged lepton of flavor l or vice-versa. The same cannot be said of NC interactions which exchange a neutral Z boson. NC interactions do not change the flavor of the incoming particles and are therefore flavor agnostic. An example of each interaction type is shown in Figure 1.2 on page 6 .

1.1.1.2 Chirality: How Neutrinos are Left Handed

Neutrinos are observed to have anti-parallel momentum vectors $\boldsymbol{P}$ to their spin vectors $\boldsymbol{\Sigma}$ and the opposite is true for anti-neutrinos. This property is called helicty and is given by (1.2)

$$\mathcal{H} = \frac{\boldsymbol{\Sigma} \cdot \boldsymbol{P}}{|\boldsymbol{P}|}. \tag{1.2}$$

While detecting neutrinos is hard as it is, the helicity is inferred from the daughter muon in charged pion decay. Since a pion has net zero (0) spin, the spin vectors of the daughters must also sum to zero. The muon from a π^+ decay has negative helicity (-1) hence the neutrino also

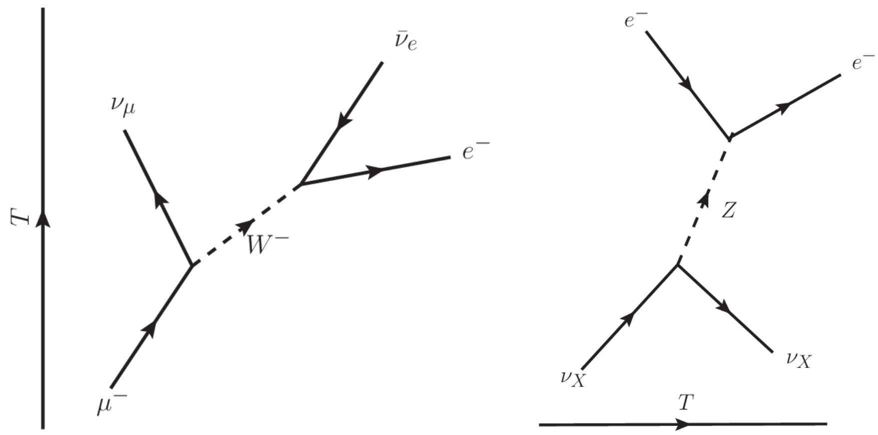

(a) Muon Decay **(b)** $\nu + e^-$ NC Scattering

Figure 1.2: Left: Muon decay $\left(\mu^- \to \nu_\mu \overline{\nu}_e e^-\right)$ Feynman diagram with time increasing from bottom to top. This is a charged current process that converts a muon into a muon neutrino via the emission of a W boson. Due to a conserved quantum number called lepton number, the W must emit an electron and electron neutrino pair. Right: Neutral current interaction Feynman diagram where time increases from left to right. This is a neutral current interaction where a neutrino of arbitrary flavor X scatters off an electron via the emission of a Z boson.

has negative helicity. To confirm the anti-neutrino's helicity is positive (+1), the interaction requires both a charge (C) conjugation and parity (P) transformation as shown in Figure 1.3 on page 7. A C conjugation is a linear transformation that transforms all particles into their corresponding antiparticles while the P transformation inverts all spatial coordinates. Thus neutrinos are referred to *left-handed* (LH) particles while anti-neutrinos are *right-handed* (RH) particles. It turns out helicity is a useful quantum number to describe neutrinos and coincides with a property called chirality. To understand chirality and its relationship to helicity requires an analysis of the Dirac Lagrangian and Dirac equation.

The Dirac Lagrangian for a free particle field $\psi(x)$ with half-integer spin can be written as

$$\mathcal{L} = \overline{\psi}(x) \left[\frac{i\hbar}{2} \sum_{\mu=0}^{3} \gamma^\mu \left(\overrightarrow{\partial_\mu} - \overleftarrow{\partial_\mu} \right) - mc \right] \psi(x) \tag{1.3}$$

where $\psi(x)$ is a four-component vector (spinor) describing a particle field and γ^μ are a set of four 4×4 matrices. The adjoint field $\overline{\psi}(x)$ is defined as

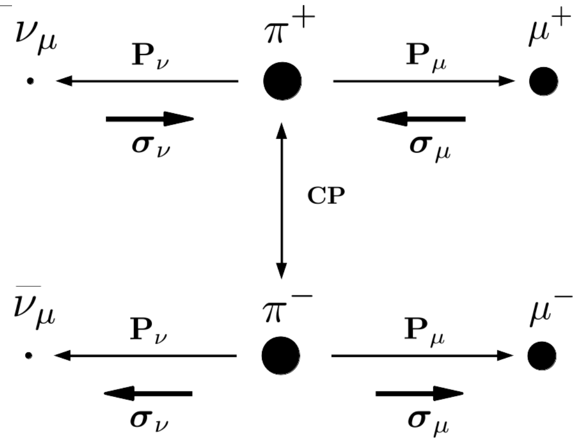

Figure 1.3: Decay of a charged pi meson into a muon and neutrino show the direction of the momentum $\boldsymbol{P}$ and spin $\boldsymbol{\sigma}$ of the outgoing particles. Since a pion at rest has zero (0) angular momentum, the system of daughter particles must have net zero angular momentum as well. A neutrino (antineutrino) is a right- (left-) handed helicity particle since its spin is (anti-)parallel to its momentum. Application of charge and parity (CP) converts all the particles into their respective antiparticles.

$$\overline{\psi}\left(x\right) \equiv \psi^{\dagger}\left(x\right)\gamma^{0} \tag{1.4}$$

where † denotes the conjugate and transpose operations. The $\overrightarrow{\partial_\mu}$ operator is a four-vector defined as

$$\partial_0 = \frac{1}{c}\frac{\partial}{\partial t}, \partial_1 = \frac{\partial}{\partial x}, \partial_2 = \frac{\partial}{\partial y}, \partial_3 = \frac{\partial}{\partial z} \tag{1.5}$$

that acts only on the right of it while $\overleftarrow{\partial_\mu}$ only acts on its left (i.e. $\overline{\psi}\overleftarrow{\partial_\mu} = \partial_\mu\overline{\psi}$). The γ^μ matrices are not unique and different representations dictate different kinematic regimes. The field equations are extracted from the Lagrangian using the Euler-Lagrange procedure. In general for a set of M fields, the field equation are given by

$$\partial_\mu \frac{\partial\mathcal{L}}{\partial\left(\partial_\mu\psi_r\right)} - \frac{\partial\mathcal{L}}{\partial\psi_r} = 0 \quad \left(r = 0, 1, 2, \ldots, M-1, M\right). \tag{1.6}$$

For the Dirac Lagrangian, the field equation for ψ is given by

$$\partial_\mu \frac{\partial\mathcal{L}}{\partial\left(\partial_\mu\overline{\psi}\right)} - \frac{\partial\mathcal{L}}{\partial\overline{\psi}} = 0 \tag{1.7}$$

which yields the Dirac equation

$$\left[i\hbar\sum_{\mu=0}^{3}\gamma^{\mu}\partial_{\mu}-mc\right]\psi\left(x\right)=0. \tag{1.8}$$

The representation of the γ^{μ} matrices that is useful to describe neutrinos is the *Chiral representation* (also called the *Weyl representation*) where

$$\gamma^{0}=\begin{bmatrix}0 & I_2\\ -I_2 & 0\end{bmatrix},\gamma^{1}=\begin{bmatrix}0 & \sigma_x\\ -\sigma_x & 0\end{bmatrix},\gamma^{2}=\begin{bmatrix}0 & \sigma_y\\ -\sigma_y & 0\end{bmatrix},\gamma^{3}=\begin{bmatrix}0 & \sigma_z\\ -\sigma_z & 0\end{bmatrix}, \tag{1.9}$$

I_2 is the 2×2 identity matrix, $\sigma_{x,y,z}$ are the Pauli Spin matrices given by

$$\sigma_x=\sigma_1=\begin{pmatrix}0 & 1\\ 1 & 0\end{pmatrix},\quad \sigma_y=\sigma_2=\begin{pmatrix}0 & -i\\ i & 0\end{pmatrix},\quad \sigma_z=\sigma_3=\begin{pmatrix}1 & 0\\ 0 & -1\end{pmatrix}.$$

Using the Chiral representation, the chirality matrix, γ^5 (the fifth gamma matrix), is defined as

$$\gamma^{5}=i\gamma^{0}\gamma^{1}\gamma^{2}\gamma^{3}=\begin{bmatrix}I_2 & 0\\ 0 & -I_2\end{bmatrix}, \tag{1.10}$$

which is diagonal as well as Hermitian meaning that its eigenvalues are real and observable. Let eigenfunctions of the chirality matrix be denoted with subscripts P and M such that the eigenvalue equations are

$$\begin{aligned}\gamma^{5}\psi_P&=+1\psi_P,\\ \gamma^{5}\psi_M&=-1\psi_M.\end{aligned} \tag{1.11}$$

The field equation solutions to (1.8) can be decomposed into ψ_P and ψ_M projections using two chiral projection operators $\hat{O}_{P,M}$ where

$$\psi=\left(\hat{O}_P+\hat{O}_M\right)\psi=\psi_P+\psi_M. \tag{1.12}$$

The chiral operators are explicitly given by

$$\hat{O}_M = \frac{1}{2}\left(I_4 - \gamma^5\right) = \begin{pmatrix} 0 & 0 \\ 0 & I_2 \end{pmatrix},$$
$$\hat{O}_P = \frac{1}{2}\left(I_4 + \gamma^5\right) = \begin{pmatrix} I_2 & 0 \\ 0 & 0 \end{pmatrix}, \tag{1.13}$$

where I_4 is the 4×4 identity matrix. Using (1.3) and (1.6), the Dirac equation becomes a set of coupled equations

$$i\hbar \sum_{\mu=0}^{3} \gamma^\mu \partial_\mu \psi_P = mc\psi_M,$$
$$i\hbar \sum_{\mu=0}^{3} \gamma^\mu \partial_\mu \psi_M = mc\psi_P \tag{1.14}$$

where dynamics are set by the mass.

Since the chiral projection operators are decompositions of the identity matrix, the simplest nontrivial solution to ψ is

$$\psi = \begin{pmatrix} \chi_P \\ \chi_M \end{pmatrix} \tag{1.15}$$

where χ represent two-component spinors. Using 1.15 the Dirac equation in (1.14) can again be rewritten as

$$i\hbar \left[\frac{1}{c}\frac{\partial}{\partial t} + \boldsymbol{\sigma} \cdot \boldsymbol{\nabla}\right] \chi_P = -mc\chi_M,$$
$$i\hbar \left[\frac{1}{c}\frac{\partial}{\partial t} - \boldsymbol{\sigma} \cdot \boldsymbol{\nabla}\right] \chi_M = -mc\chi_P, \tag{1.16}$$

where

$$\boldsymbol{\sigma} \cdot \boldsymbol{\nabla} = \sigma_x \frac{\partial}{\partial x} + \sigma_y \frac{\partial}{\partial y} + \sigma_z \frac{\partial}{\partial z}. \tag{1.17}$$

In the limiting case of vanishing mass ($m \to 0$), as is in the SM, the free particle field equations in (1.16) decouple into

$$\left(\frac{E}{c} + \boldsymbol{\sigma} \cdot \boldsymbol{P}\right) \chi_P = 0,$$
$$\left(\frac{E}{c} - \boldsymbol{\sigma} \cdot \boldsymbol{P}\right) \chi_M = 0, \tag{1.18}$$

where the differential operators have been expressed as energy E and momentum three-vector $\boldsymbol{P}$. For massless neutrinos, χ_P and hence ψ_P, describe particles of negative energy $E = -|\boldsymbol{P}|\, c$ which in the context of quantum field theory are interpreted as antiparticles traveling backwards in time. Conversely, ψ_M have positive energy $E = |\boldsymbol{P}|\, c$ and which means they are particles traveling forward in time.

If one also multiplies (1.14) by $\gamma^5\gamma^0$ and using the fact that the spin operator $\boldsymbol{\Sigma}$ is

$$\boldsymbol{\Sigma} = i\left(\gamma^2\gamma^3, \gamma^3\gamma^1, \gamma^1\gamma^2\right) = \gamma^0\gamma^k\gamma^5 \quad (k = 1, 2, 3) \tag{1.19}$$

each decoupled equation becomes after some manipulation

$$\frac{\boldsymbol{\Sigma}\cdot\boldsymbol{P}}{|\boldsymbol{P}|}\psi_{P,M} = \gamma^5\psi_{P,M} = \pm\psi_{P,M}, \tag{1.20}$$

where one recognizes that helicity and chiral states are the same ($m \to 0$ only). Thus the labels M and P actually are identical to the LH and RH helicity labels, respectively, given ealier. Using the results from before, a neutrino is always observed as a LH particle while the anti-neutrino is always observed as a RH antiparticle.

The observation of only LH neutrinos and RH anti-neutrinos is an important feature in the SM. However, since neutrinos are known to have mass from oscillations, it is theoretically possible to observe a RH neutrino and LH anti-neutrino. That would require boosting to a highly relativistic reference frame with respect to the laboratory.

The free neutrino field is a construction of a vector minus axial vector, also referred to as V-A, as shown in (1.12) and (1.13). This feature is what allows for the weak force to violate P-symmetry and CP-symmetry. Further observation of CP violation is being explored with neutrinos through a process called neutrino oscillations. This will be explained in the next subsection.

1.1.2 Neutrino Oscillations

Neutrino oscillations are the observation of a neutrino produced of definite flavor and later observed as a different flavor. This phenomenon was first observed as a deficit of neutrinos for a number of atmospheric and solar neutrino experiments. The deficit also seemed more pronounced for atmospheric neutrinos as the distance from their source increased. For neutrino oscillations to occur, at least one neutrino must be massive. This observation firmly established that the SM is wrong with its prediction of massless neutrinos

The first indication of neutrino oscillations was from the Ray Davis Homesteak Mine experiment which began in the 1960s. Ray Davis was an expert Chemist and designed a radiochemical experiment to measure the flux of neutrinos from Sun. The purpose of this experiment was to test John Bahcall's prediction of the fusion rate in the Sun and neutrino flux from it as well. Davis' experiment would need to operate for many years to collect enough statistics due to expected low capture rate. Measurements continued into the 1980s and showed that the flux of neutrinos as measured at Homesteak was about 1/3 the expected rate and became known as the "Solar Neutrino Problem." The primary solutions were either the the solar model was incorrect or the neutrino capture cross section is incorrect somehow. The Sudbury Neutrino Observatory (SNO) was able to resolve this problem by making a model-independent measurement of the solar neutrino flux. SNO observed a ν_eCC-to-NC ratio of 0.301 ± 0.033, which confirmed that only about 30% of neutrinos arrive as ν_e flavors on Earth. Saying this another way, the majority of neutrinos arrive as the wrong flavor [21].

Another outstanding problem emerged with measurements of atmospheric neutrinos, in particular muon and electron types. Atmospheric neutrinos are produced when high energy cosmic rays strike atmospheric particles. These cosmic ray collisions generate mostly pions and kaons that decay into neutrinos. When trying to measure the ν_μ/ν_e ratio and comparing that with expected ratio, there was another significant deficit. This was particularly a problem as a function of the zenith angle for the Super-Kamiokande (SK) experiment. SK is a 50kt tank of pure water lined with thousands of photomultiplier tubes designed to observe solar and atmospheric neutrinos. It was the first experiment to perform a neutrino oscillation analysis that successfully explained the deficit.

While the phenomenon of neutrino oscillations has been understood for decades, it is not incorporated formally into the SM since oscillations require the neutrino has mass. The reasons why neutrino oscillations require massive neutrinos is explained in the next subsection.

1.1.2.1 Two Flavor Derivation

The phenomenon of neutrino oscillations can be described with elementary, non-relativistic Quantum Mechanics. Beginning with the Schrödinger Equation in (1.21)

$$-\frac{\hbar}{i}\frac{\partial}{\partial t}\left|\nu(\mathbf{r},t)\right\rangle = \hat{H}\left|\nu(\mathbf{r},t)\right\rangle, \tag{1.21}$$

where $\hat{H}$ is the Hamiltonian for the physical system, one considers a massive neutrino of mass m_j in its rest frame (free particle). The Hamiltonian is diagonal in this case, which acting on $\left|\nu_j\right\rangle$ results in the eigenvalue equation

$$\hat{H}\left|\nu_j(\mathbf{r},t)\right\rangle = E_j\left|\nu_j(\mathbf{r},t)\right\rangle, \tag{1.22}$$

where E_j is the energy of the neutrino $\left|\nu_j\right\rangle$. Substituting (1.22) into (1.21) and solving for $\left|\nu(\mathbf{r},t)\right\rangle$, one obtains the following

$$\left|\nu_j(\mathbf{r},t)\right\rangle = e^{-iE_jt/\hbar}\left|\nu_j(\mathbf{r},t=0)\right\rangle, \tag{1.23}$$

where $\left|\nu_j(\mathbf{r},t=0)\right\rangle$ is created with momentum $\mathbf{p}$ at the origin $\mathbf{r}=0$. The time-independent solution to (1.21) is a plane-wave given by

$$\left|\nu_j(\mathbf{r},t=0)\right\rangle = e^{i\mathbf{p}\cdot\mathbf{r}/\hbar}\left|\nu_j\right\rangle. \tag{1.24}$$

Before being able to describe neutrino oscillations, we must define our basis states. For this example, consider that there are only two eigenstates, labeled ν_1 and ν_2, in the "mass" basis with definite mass m_1 and m_2, respectively. However, experiments can produce neutrinos, as well as probe them, only of definite "flavor", denoted by a Greek letter subscript λ. Let the generated neutrino, which is a linear superposition of mass states 1 and 2, have momentum $\mathbf{p}$ and flavor α. Since both mass eigenstates share the same momentum momentum $\mathbf{p}$ (but not energy!), the exponential term in (1.24) is an overall phase that will cancel out later. One can postulate a linear transformation, U, between the basis states given by (1.25).

$$\begin{bmatrix} \nu_\alpha \\ \nu_\beta \end{bmatrix} = \begin{bmatrix} U_{11} & U_{12} \\ U_{21} & U_{22} \end{bmatrix} \begin{bmatrix} \nu_1 \\ \nu_2 \end{bmatrix} \tag{1.25}$$

This linear transformation must be a unitary matrix $\left(U^{-1} = U^\dagger, \dagger = \text{transpose conjugate}\right)$ since the states $\nu_{1,2}$ constitute a complete orthonormal basis in the mass basis. With this unitary property, we can imagine U as a rotation matrix

$$\begin{bmatrix} \nu_\alpha \\ \nu_\beta \end{bmatrix} = \begin{bmatrix} \cos(\theta) & \sin(\theta) \\ -\sin(\theta) & \cos(\theta) \end{bmatrix} \begin{bmatrix} \nu_1 \\ \nu_2 \end{bmatrix}, \tag{1.26}$$

where θ is the angle between the two bases. One can imagine this transformation between bases as shown in Figure 1.4 on page 14 . Creating a neutrino of flavor α and observe it after a time $t = T > 0$, the probability of observing it as flavor $\beta \neq \alpha$ is given by

$$\begin{aligned} \mathcal{P}\left(\nu_\alpha \to \nu_\beta\right) &= \left|\langle \nu_\alpha(t=0) | \nu_\beta(t=T)\rangle\right|^2 \\ &= |(\cos(\theta)\, \langle \nu_1(t=0)| + \sin(\theta)\, \langle \nu_2(t=0)|) \\ &\quad \times (-\sin(\theta)\, |\nu_1(t=T)\rangle + \cos(\theta)\, |\nu_2(t=T)\rangle)|^2 \\ &= |\langle \nu_1(0)|\nu_1(T)\rangle\, (-cs) + \langle \nu_1(0)|\nu_2(T)\rangle\, (cc) \\ &\quad + \langle \nu_2(0)|\nu_1(T)\rangle\, (-ss) + \langle \nu_2(0)|\nu_2(T)\rangle\, (sc)|^2 \end{aligned} \tag{1.27}$$

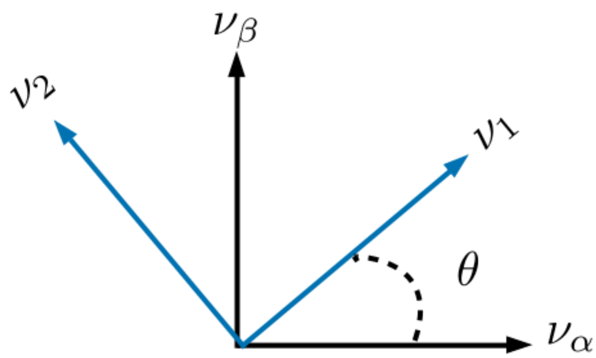

Figure 1.4: The depiction of two neutrino flavor change of basis using a rotation matrix. Compare this with (1.26).

where for simplicity $c = \cos(\theta)$ and $s = \sin(\theta)$. Evaluating all inner products and simplifying terms in (1.27) results in (1.28) below.

$$\mathcal{P}\left(\nu_\alpha \to \nu_\beta\right) = \sin^2(2\theta)\sin^2\left(\frac{E_1 - E_2}{2\hbar}T\right) \tag{1.28}$$

The terminology of "neutrino oscillations" should be more apparent now since (1.28) demonstrates that the probability changes sinusoidally. This equation is not, however, terribly useful in the laboratory frame since it is hard to make an experiment where the travel time an individual neutrino is well known. Instead, one can make useful approximations that are accessible in the laboratory frame. Since neutrinos are nearly massless, they travel very close to the speed of light. Therefore we can replace time T with L/c where L is the distance between the neutrino origin and detection and c is now the speed of light in vacuum. One can also approximate the energy of the mass eigenstate as

$$\begin{aligned} E_j = \left(m_j^2c^4 + p_j^2c^2\right)^{\frac{1}{2}} &= p_jc\left(1 + \frac{m_j^2c^2}{p_j^2}\right)^{\frac{1}{2}} \\ &\approx p_jc\left(1 + \frac{m_j^2c^2}{2p_j^2} + \mathcal{O}\left(\frac{m_jc}{p_j}\right)^4\right) \\ &\approx E_\nu + \frac{m_j^2c^4}{2E_\nu}, \end{aligned} \tag{1.29}$$

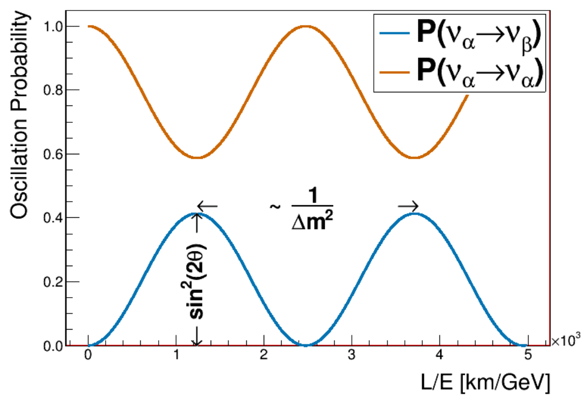

Figure 1.5: Two flavor oscillation probability as a function L/E is shown using $\theta = 20^{\circ}$ and $\Delta m^2 = [\ 10^{-3}]eV^2$. The spacing between adjacent peaks/troughs is proportional to the inverse of Δm^2. Note that $\mathcal{P}\left(\nu_\alpha \to \nu_\alpha\right) = 1 - \mathcal{P}\left(\nu_\alpha \to \nu_\beta\right)$ since the oscillation probability must always sum to 1.

where for experiments $p_j \gg m_j c$ and $p_j c \approx E_\nu$ where E_ν is the neutrino energy as measured in the laboratory. Substituting the assumptions in (1.28), the oscillation probability is given by

$$\mathcal{P}\left(\nu_\alpha \to \nu_\beta\right) = \sin^2(2\theta)\sin^2\left(\frac{\Delta m^2 c^3}{4\hbar}\frac{L}{E_\nu}\right), \tag{1.30}$$

where $\Delta m^2 = m_2^2 - m_1^2$ is the mass-squared difference between the mass states. For a momentum consider evaluating all the physical constants in natural units ($c = \hbar = 1$). An appropriate choice of units for Δm^2, L, and E_ν results in

$$\mathcal{P}\left(\nu_\alpha \to \nu_\beta\right) = \sin^2(2\theta)\sin^2\left(1.27\frac{\Delta m^2}{\left[\mathrm{eV}^2\right]}\frac{L/E_\nu}{\left[\mathrm{km}/\mathrm{GeV}\right]}\right)\ \text{[natural units]} \tag{1.31}$$

which more clearly demonstrates the Physics in neutrino oscillations. The oscillation probability has an amplitude of $\sin^2(2\theta)$ and varies with frequency inversely proportional to Δm^2 as illustrated in Figure 1.5 on page 15 . Since L and E_ν are the only controllable parameters for an oscillation experiment, probing θ or Δm^2 can be difficult unless the experiment can probe a large range of L/E_ν as shown in Figure 1.6 on page 16 .

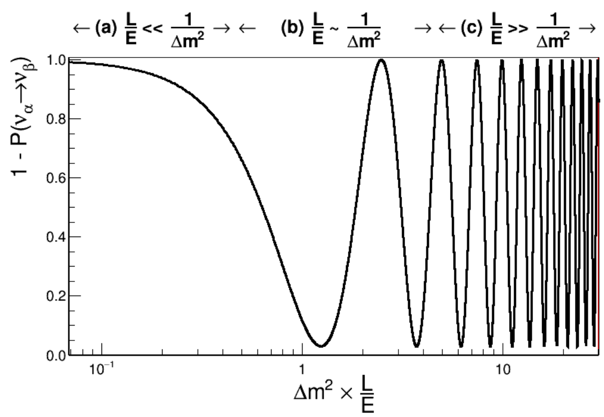

Figure 1.6: Logarithmic plot of the survival probability $\left(1 - \mathcal{P}\left(\nu_\alpha \to \nu_\beta\right) = \mathcal{P}\left(\nu_\alpha \to \nu_\alpha\right)\right)$ over a wide range of L/E values for $\theta = 40^\circ$. The arrows above the plot roughly denote three possible cases: (a) no oscillations ($L/E \ll 1/\Delta m^2$); (b) sensitivity to oscillations ($L/E \sim 1/\Delta m^2$); (c) only average measurement ($L/E \gg 1/\Delta m^2$). Image originally inspired by [17].

1.1.2.2 Three Flavor Oscillations

In the general case of oscillations using a $n \times n$ mixing matrix, the unitary transformation can be written as a rotation matrix with $\frac{n}{2}(n-1)$ weak mixing angles with $\frac{1}{2}(n-2)(n-1)$ Charge-Parity (CP) violating phases. In addition, oscillations are dictated by a total of $n-1$ mass-squared splittings [21]. This all assumes that neutrinos obey the Dirac Equation, or that they are not their own antiparticles. The flavored mixing model is the 3×3 matrix since there are three known neutrino flavors, ν_e, ν_μ, and ν_τ, which means there are three (3) mixing angles, one (1) CP violating phase, and two (2) mass-squared splittings.

The most frequently used matrix parameterization is the MNSP (MNSP: Maki-Nakagawa-Sakata-Pontecorvo) matrix. Pontecorvo is accredited for first conceiving of neutrino oscillations, albeit between neutrino and anti-neutrinos [14]. It was Maki, Nakagawa, and Sakata who conceived of the parameterization based off the ideas of Pontecorvo [13]. The MNSP matrix is decomposed into separate rotation matrices as given by (1.32)

Source	Species	Baseline [km]	Mean Energy [GeV]	$\min\left(\Delta m^2\right)$ [eV^2]
Reactor	$\overline{\nu}_e$	1	$\sim 10^{-3}$	$\sim 10^{-3}$
Reactor	$\overline{\nu}_e$	100	$\sim 10^{-3}$	$\sim 10^{-5}$
Accelerator	$\nu_\mu, \overline{\nu}_\mu$	1	~ 1	~ 1
Accelerator	$\nu_\mu, \overline{\nu}_\mu$	10^3	~ 1	$\sim 10^{-3}$
Atmospheric ν's	$\nu_{e,\mu}, \overline{\nu}_{\mu,e}$	10^4	~ 1	$\sim 10^{-4}$
Sun	ν_e	1.5×10^8	$\sim 10^{-3}$	$\sim 10^{-11}$

Table 1.1: Sensitivity of different oscillation experiments originally published in [19].

$$U_{\mathrm{MNSP}} = \overbrace{\begin{bmatrix} 1 & 0 & 0 \\ 0 & c_{32} & s_{32} \\ 0 & -s_{32} & c_{32} \end{bmatrix}}^{U_{\mathrm{atm}}} \times \overbrace{\begin{bmatrix} c_{31} & 0 & s_{31}e^{i\delta_{\mathrm{CP}}} \\ 0 & 1 & 0 \\ -s_{31}e^{-i\delta_{\mathrm{CP}}} & 0 & c_{31} \end{bmatrix}}^{U_{\mathrm{rea}}} \times \overbrace{\begin{bmatrix} c_{21} & s_{21} & 0 \\ -s_{21} & c_{21} & 0 \\ 0 & 0 & 1 \end{bmatrix}}^{U_{\mathrm{sol}}} \tag{1.32}$$

where

$$c_{ij} = \cos\theta_{ij}, s_{ij} = \sin\theta_{ij}, \tag{1.33}$$

and δ_{CP} represents the CP violating phase. Each rotation matrix represents the different sources for neutrino oscillations experiments with "atm", "rea", and "sol" representing atmospheric ν's, nuclear reactor ν's, and Solar ν's, respectively. The sensitivity of neutrino oscillations for different sources is given in Table 1.1 on page 17.

If neutrinos are their own antiparticles, they do not follow the Dirac Equation but do follow the Majorana Equation. This adds two (in general $n-1$) more CP violating phases to the MNSP matrix in (1.32)

$$U_{\mathrm{MNSP}} \to U_{\mathrm{MNSP}} \times \overbrace{\begin{bmatrix} 1 & 0 & 0 \\ 0 & e^{i\alpha} & 0 \\ 0 & 0 & e^{i\beta} \end{bmatrix}}^{U_{\mathrm{Majorana}}} \tag{1.34}$$

Unfortunately, neutrino oscillations are not able to probe the Majorana phases since the Majorana matrix is diagonal. The question of if neutrinos are Majorana ($\nu = \overline{\nu}$) or Dirac

($\nu \neq \overline{\nu}$) particles is an open question and is being explored by non-oscillation experiments. The full three flavor oscillation probability is given by

$$\begin{aligned}\mathcal{P}\left(\nu_\alpha \to \nu_\beta\right) = \delta_{\alpha\beta} - 4\sum_{j=1}^{3}\left[\sum_{i>j}^{3}\mathrm{Re}\left(K_{\alpha\beta,ij}\right)\sin^2\left(\phi_{ij}\right)\right] \\ +4\sum_{j=1}^{3}\left[\sum_{i>j}^{3}\mathrm{Im}\left(K_{\alpha\beta,ij}\right)\sin\left(\phi_{ij}\right)\cos\left(\phi_{ij}\right)\right]\end{aligned} \tag{1.35}$$

where

$$K_{\alpha\beta,ij} = U_{\alpha i}U^*_{\beta_i}U^*_{\alpha j}U_{\beta j} \tag{1.36}$$

encapsulates the MNSP matrix elements and

$$\phi_{ij} = \frac{\Delta m^2_{ij}c^3}{4\hbar}\frac{L}{E_\nu}. \tag{1.37}$$

Since CP violation means that $\mathcal{P}\left(\nu_\alpha \to \nu_{\beta\neq\alpha}\right) \neq \mathcal{P}\left(\overline{\nu}_\alpha \to \overline{\nu}_{\beta\neq\alpha}\right)$, CP violating (conserving) terms must be an odd (even) function of δ_{CP}. Consider the following examples, muon neutrino disappearance and muon neutrino to electron neutrino appearance.

Muon Neutrino Disappearance The probability of a muon type neutrinos disappearing is given by

$$\begin{aligned}\mathcal{P}\left(\overset{(-)}{\nu}_\mu \to \overset{(-)}{\nu}_\mu\right) = 1 - 4s^2_{23}c^2_{13}\left(V_{\cos\delta_{\mathrm{CP}}}\right)\sin^2\phi_{31} \\ -4s^2_{23}c^2_{13}\left(Z_{\cos\delta_{\mathrm{CP}}}\right)\sin^2\phi_{32} \\ -4\left(V_{\cos\delta_{\mathrm{CP}}}\right)\left(Z_{\cos\delta_{\mathrm{CP}}}\right)\sin^2\phi_{21}\end{aligned} \tag{1.38}$$

where

$$V_{\cos\delta_{\mathrm{CP}}} = s^2_{12}c^2_{23} + s^2_{13}s^2_{23}c^2_{12} + 2s_{12}s_{13}s_{23}c_{12}c_{23}\cos\delta_{\mathrm{CP}} \tag{1.39}$$

$$Z_{\cos\delta_{\mathrm{CP}}} = c^2_{12}c^2_{23} + s^2_{13}s^2_{23}s^2_{12} - 2s_{12}s_{13}s_{23}c_{12}c_{23}\cos\delta_{\mathrm{CP}} \tag{1.40}$$

and $\overset{(-)}{\nu}_\mu$ represents either ν_μ or $\overline{\nu}_\mu$. Since all CP violating terms in (1.38) are even functions of δ_{CP}, this channel does not offer insights into CP violation in a vacuum[4].

Electron Neutrino Appearance While CP violation is not observable in muon neutrino disappearance, it is with electron neutrino appearance. The appearance probability of electron neutrinos types from muon types is given by

$$\begin{aligned}\mathcal{P}\left(\overset{(-)}{\nu}_\mu \rightarrow \overset{(-)}{\nu}_e\right) =& 4c_{13}^2 s_{13}^2 s_{23}^2 \sin^2\phi_{31} \\ &+ 8\left(X_{\cos\delta_{\mathrm{CP}}}\right)\cos\phi_{23}\sin\phi_{31}\sin\phi_{21} \\ &\overset{(+)}{-} 8\underbrace{\left(Y_{\sin\delta_{\mathrm{CP}}}\right)}_{\text{CP violating}}\sin\phi_{32}\sin\phi_{31}\sin\phi_{21} \\ &+ 4\left(Z_{\cos\delta_{\mathrm{CP}}}\right)s_{12}^2 c_{13}^2\sin^2\phi_{21}\end{aligned} \tag{1.41}$$

where

$$X_{\cos\delta_{\mathrm{CP}}} = c_{13}^2 s_{12} s_{13} s_{23}\left(c_{12}c_{23}\cos\delta_{\mathrm{CP}} - s_{12}s_{13}\right) \tag{1.42}$$

$$Y_{\sin\delta_{\mathrm{CP}}} = \frac{1}{8}\sin\left(2\theta_{12}\right)\sin\left(2\theta_{13}\right)\sin\left(2\theta_{23}\right)c_{13}\sin\delta_{\mathrm{CP}} \tag{1.43}$$

and (+) represents the sign change from neutrinos to anti-neutrinos. The CP violating term (1.43) is also known as the Jarlskog Invariant and is a measure of CP violation independent of the mixing parameterization [12]. This oscillation channel are of primary importance in accelerator and atmospheric neutrino oscillation experiments.

Current and next generation experiments aim to improve knowledge of the mixing parameters. There are a couple of degeneracies to unravel as well as precise measurement of δ_{CP}. While the two defined mass-squared splittings $\Delta m_{21}^2 = \Delta m_{\mathrm{sol}}^2$ and $\Delta m_{32}^2 = \Delta m_{\mathrm{atm}}^2$ are known, it is unknown which eigenstates are more massive. This problem is known as the mass hierarchy problem and is illustrated in Figure 1.7a on page 20. Normal hierarchy refers to the case where $m_3 > m_2 > m_1$whereas the inverted hierarchy has $m_2 > m_1 > m_3$.

[4]When going to through matter however, the oscillation probability is affected. This is explained more in Section 1.1.2.3.

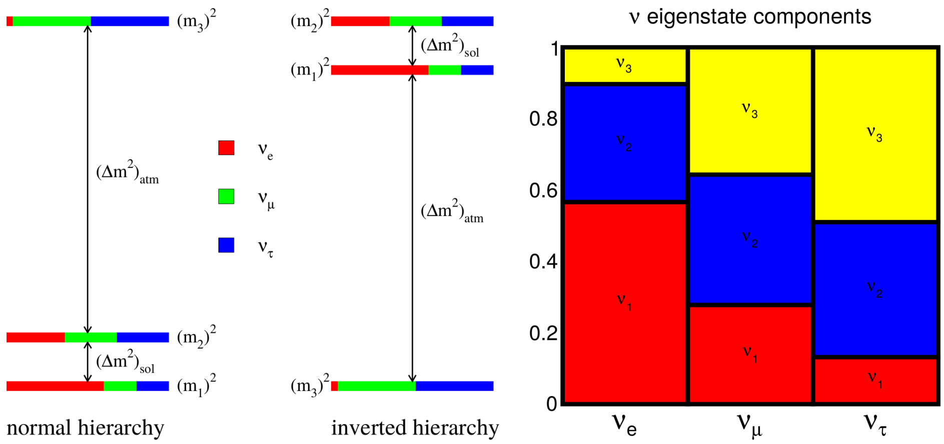

(a) Mass hierarchy as shown in [7]

(b) Mass eigenstate components as shown in [4]

Figure 1.7: Left: the mass hierarchy problem is such that while the solar and atmospheric mixing mass-squared differences are clearly defined, the absolute mass scale is unknown. Since $m_2 > m_1$ by definition, it is currently unknown if m_3 is more or less massive than m_2, or even massless! Notice the colored bars for each mass eigenstate which corresponded to the approximate flavor content of the neutrino. For example, state "2" has about equal three portions of all three flavors. Right: the mass eigenstate components of each flavor eigenstate. This is a complementary demonstration of the MNSP matrix.

Also knowledge if θ_{23} is in the first octant $\theta \in (0, \pi/2)$ or second octant $\theta \in (\pi/2, \pi/4)$ requires large statistics. Finally the value of δ_{CP} is quite uncertain with values in the 3rd and 4th quadrants. Best fit measurements of the oscillations parameters is given in Table 1.2 on page 21 .

1.1.2.3 Matter Effects

Traveling through matter also increases the sensitivity of oscillation measurements. Known as the Mikheyev-Smirnov-Wolfenstein (MSW) effect, all oscillations are affected by coherent forward scattering of neutrinos with electrons in the media. Taking the example of $\overset{(-)}{\nu}_\mu \to \overset{(-)}{\nu}_e$ from (1.38), the MSW effect to first order is

Parameter	Normal Hierarchy value	Inverted Hierarchy value	Units
$\Delta m^2_{32} = \Delta m^2_{\text{atm}}$	2.51 ± 0.05	-2.56 ± 0.04	10^{-3} eV^2
$\Delta m^2_{21} = \Delta m^2_{\text{sol}}$	7.53 ± 0.18		10^{-5} eV^2
$\sin^2(\theta_{21})$=$\sin^2(\theta_{\text{sol}})$	$0.307^{+0.013}_{-0.012}$		1
$\sin^2(\theta_{32})$=$\sin^2(\theta_{\text{atm}})$	O1: $0.417^{+0.025}_{-0.028}$ O2: $0.597^{+0.024}_{-0.030}$	O1: $0.421^{+0.033}_{-0.025}$ O2: $0.592^{+0.023}_{-0.030}$	1
$\sin^2(\theta_{31})$	2.12 ± 0.08		10^{-2}
δ_{CP}	217^{+40}_{-28}	280^{+25}_{-28}	degrees

Table 1.2: Table of best fit MNSP parameters split by normal and inverted hierarchy. O1 and O2 correspond to the first octant ($\theta \in (0, \pi/2)$) or second octant ($\theta \in (\pi/2, \pi/4)$). All values except for δ_{CP} are combined values from the Particle Data Group and δ_{CP} is from the 2018 NuFit analysis [8, 19].

$$\begin{aligned}\mathcal{P}\left(\overset{(-)}{\nu}_\mu \rightarrow \overset{(-)}{\nu}_e\right) \rightarrow & \mathcal{P}\left(\overset{(-)}{\nu}_\mu \rightarrow \overset{(-)}{\nu}_e\right) + \frac{8\alpha}{\Delta m^2_{31}}\left(c^2_{13}s^2_{13}s^2_{23}\right)\left(1 - 2s^2_{13}\right) \\ & \times \left(\sin^2\phi_{31} \overset{(+)}{-} \underbrace{\left(\frac{\Delta m^2_{31}c^3}{4\hbar}\frac{L}{E_\nu}\right)}_{\phi_{31}} \cos\phi_{32}\sin\phi_{31}\right)\end{aligned} \tag{1.44}$$

where

$$\alpha = 2\sqrt{2}G_F n_e E_\nu \tag{1.45}$$

and G_F is the Fermi constant and n_e is the average electron density of the Earth which the neutrinos travel [5]. Carefully studying 1.44 reveals that the MSW effect alters the oscillation probability as a function of the electron density and increases in magnitude with baseline.

1.1.3 CP Violation: Origins of Matter

To conclude the introduction on neutrinos, lets briefly examine the implications of CP violation. The observation of CP violation in the lepton sector might provide critical insight into the origins of the matter. CP violation dictates that certain interactions behave differently between matter or antimatter like $\mathcal{P}\left(\nu_\mu \rightarrow \nu_e\right) \neq \mathcal{P}\left(\overline{\nu}_\mu \rightarrow \overline{\nu}_e\right)$. The Big Bang Theory suggests that in the first fractions of a second of the Universe, equal amounts of matter and antimatter were created. However, observational evidence shows the Universe consists of baryonic matter (i.e. protons and neutrons). This is known as the Baryon Asymmetry of the Universe (BAU).

The process of Baryogenesis[5] is a favored model to explain the BAU and lacks a necessary precursor mechanism. One of the necessary conditions for Baryogenesis [16] is C symmetry violation and CP violation. Evidence of CP violation has been experimentally confirmed in the quarks, but not to the level which resolves the BAU. Baryogenesis can be achieved by having Leptogenesis[6] occur first through the decay of very heavy, right handed Majorana neutrino ($\nu = \overline{\nu}$) through the *see-saw* mechanism. Detailed discussions on Leptogenesis and the *see-saw* mechanism can found in [4].

1.2 Tokai-to-Kamioka Experiment

The Tokai-to-Kamioka (T2K) experiment is a long baseline, neutrino oscillation experiment hosted in Japan [1] as shown in Figure 1.8 on page 23. It is the successor experiment to the KEK-to-Kamioka neutrino oscillation experiment also hosted in Japan. T2K produces its high intensity, muon neutrino pure beam at the Japan Proton Accelerator Complex (J-PARC), a world class particle accelerator facility. The beam is directed at the Super-

[5] Baryogenesis is the mechanism by which matter and antimatter baryons are created in the early Universe.

[6] Leptogenesis is the mechanism by which leptons and anti-leptons are created in the early Universe.

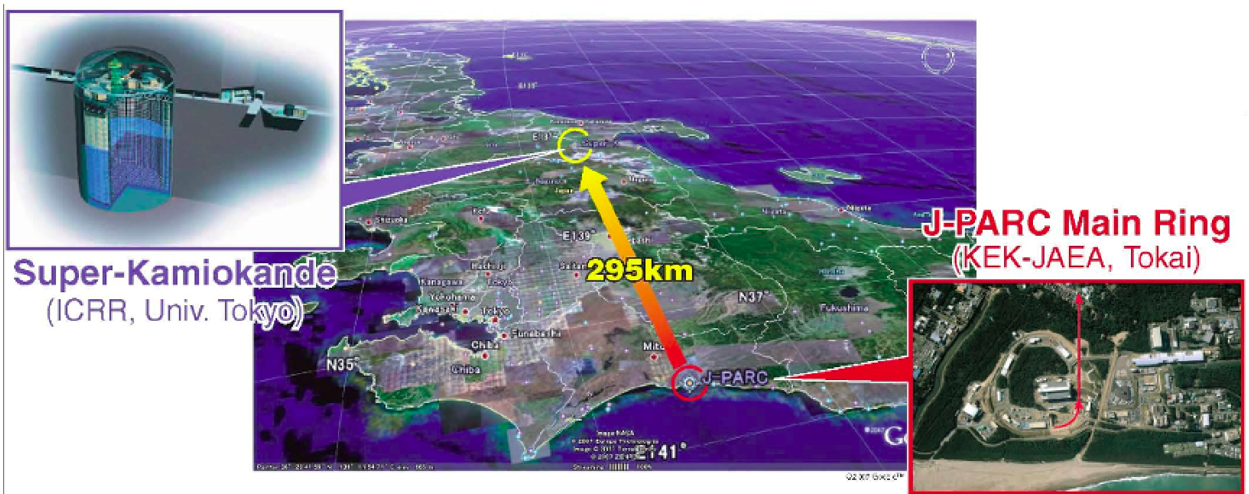

Figure 1.8: Birds eye view of the T2K experiment on the Japanese archipelago. An intense beam of neutrinos are produced at the J-PARC site (bottom right red box) using high energy protons. The beam is directed towards the Super-Kamiokande detector (top left blue box) at a distance of 295 km away from J-PARC.

Kamiokande (SK) [10] detector which is 295 km away from the source. Along the beamline at 280m from the beam source are a series of near detectors called ND280 [9] to observe and characterize the unoscillated beam. The beam is designed to maximize the $\nu_\mu \to \nu_e$ probability at the 295km baseline using a neutrino energy spectrum sharply peaked at 0.6GeV. This spectrum is achieved by directing the center of the beam 2.5 degrees from SK.

T2K was primarily designed to measure the last unknown MNSP mixing angle θ_{13}, which was thought to be nearly zero. In addition it set out to measure to high precision the atmospheric mixing parameters, θ_{23} and Δm^2_{23}. One of its early successes was a landmark 7.3σ measurement of a non-zero θ_{13} using the electron-neutrino appearance measurement [2]. It continues to be a world leader in oscillation physics and as of 2018 rejects CP conserving values ($\delta_{\mathrm{CP}} = 0, \pi$) at the 2σ level [3].

The following topics will be discussed in the following order. First a look how neutrinos are produced at J-PARC. Next a detailed look at the T2K near detectors which are used in this thesis. This is followed by a discussion on Super-Kamiokande, the T2K far detector. The final topic is the basics of an oscillation analysis using a near and far detector.

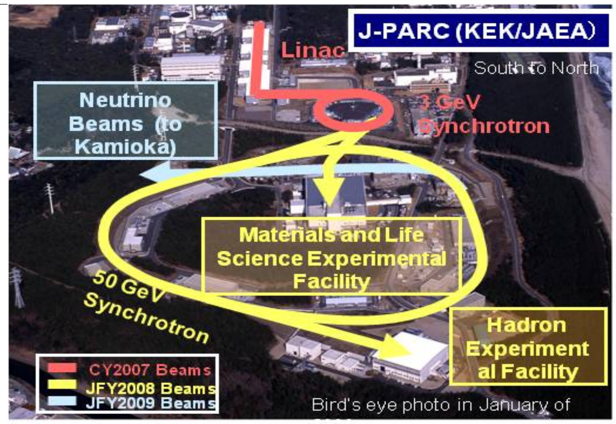

Figure 1.9: Bird's eye view of the J-PARC center showing the primary components of its accelerator programs. To generate the high intensity neutrino beam, first the linear accelerator (Linac, red) accelerates hydrogen ions (protons) into the 3 GeV Synchrotron (also red) called the rapid-cycle synchrotron (RCS). The RCS then injects some of its protons into the 50 GeV Sychrotron (yellow) called the main ring (MR) which currently runs at 30 GeV. Finally the MR protons are directed into a target material along the neutrino beamline (teal) [6].

1.2.1 Neutrino Production at J-PARC

To facilitate the high intensity neutrino beam requirements for T2K, the J-PARC site generates a high intensity proton beam through a series of particle accelerators. A bird's eye view of J-PARC can be seen in Figure 1.9 on page 24 which highlights its different accelerators and facilities. For this section, note that all beam energies are kinetic energies.

Protons for the T2K beamline are first accelerated in the J-PARC linear accelerator[7] (linac) and rapid cycle synchrotron[8] (RCS). Protons are initially extracted from a hydrogen ion ($^1_1H^+$) source. Those protons are feed through a radio frequency (RF) quadropole magnet and a series of linac elements as shown in 1.10a. Each linac element accelerates the protons using carefully coordinated oscillating electric fields generated by RF pulses. After travelling 240m along the linac, the protons are boosted to 400 MeV and transported into the RCS. The 348m circumference RCS then further boosts the protons to 3 GeV at an operating

[7]A linear accelerator accelerates particles using time varying electric fields along a one direction, terminal beamline. Not only used in particle physics, they are also used in the medical field to generate X-rays.

[8]A synchrotron is cyclic particle accelerator that relies on time varying magnetic fields to accelerate particles. Since they require many magnets and large spaces to operate, they are usually operated at national laboratories for others uses as well like material and life sciences.

frequency of 25 Hz. While being accelerated, protons are aggregated into two bunches and focused using particle collimators as shown in Figure 1.10b on page 26.

The next stage for the protons intended for the neutrino beamline is the much larger main ring (MR) synchrotron as shown in Figure 1.10c on page 26 which has a circumference of 1567m. While nominally designed to boost protons to 50 GeV, it currently operates at 30 GeV. Protons are injected into the MR to form eight proton bunches (spill), initially six when T2K first ran, before entering the neutrino beamline. The total temporal width of the spill is approximately 0.5μs. [1]. At a spill cycle frequency of 0.5Hz, the bunches are extracted from the MR into the neutrino beamline.

The neutrino beamline is designed to direct the protons toward SK and generate neutrinos by impinging them on a cylindrical target. Figure 1.11a on page 27 shows the process of proton extraction from the MR for both primary and secondary neutrino beamlines. In the primary beamline, a series of normal and superconducting magnets steer the proton beam 80.7° along a 104m radius of curvature. The secondary beamline, better shown in Figure 1.11b on page 27, illustrates the production of neutrinos. The beam spill impinges on a graphite target at the target station, which produces high energy pions like those produced from cosmic ray collisions in the upper atmosphere. To enhance the flux of neutrinos, a series of current pulsed, focusing magnets called horns[9] as shown in Figure 1.11c on page 27 are used to focus pions of the correct charge towards SK. The horns are pulsed at +250kA (-250kA) to select positively (negatively) charged pions. The focused pions are allowed to decay along a 96m long decay volume to boost the daughter neutrinos along the beamline direction. The decay volume needs to be as close to vacuum as possible to reduce pion absorption and among other reasons, and thus it is filled with gaseous helium at 1 atm for safety reasons. Daughter muons of sufficient momentum ($>$ 5 GeV) are further used to characterize the neutrino flux .

[9]The name horn derives from the fact that the focusing magnets are shaped like brass horns in a music ensemble or marching band. One can think of these horns like a focusing lens for charged particles.

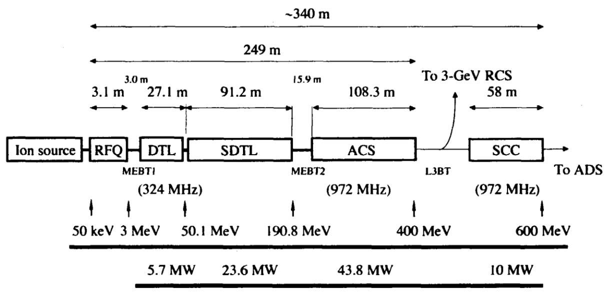

(a) 400 MeV linac

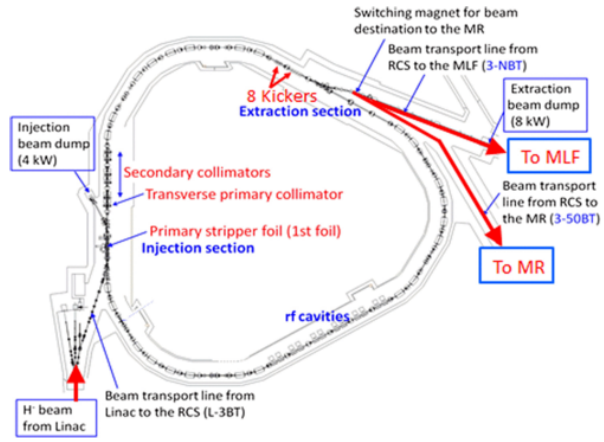

(b) 3 GeV RCS

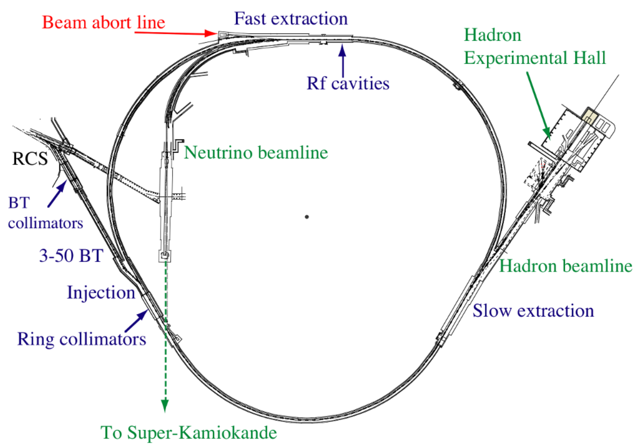

(c) 50 GeV MR

Figure 1.10: Schematics of the J-PARC accelerators. (a) The linac accelerates protons to 400 MeV of kinetic energy from the ion source through linear accelerator (linac) elements [20]. (b) Protons from the linac are collected into the rapid cycle synchrotron (RCS) and accelerated to 3 GeV [15]. (c) Protons from the RCS are injected into the main ring (MR) synchroton which further accelerates the protons. While the MR is designed for 50 GeV, it currently operates at 30 GeV. For T2K, the protons are bunched in the MR and extracted into the "Neutrino beamline" [11].

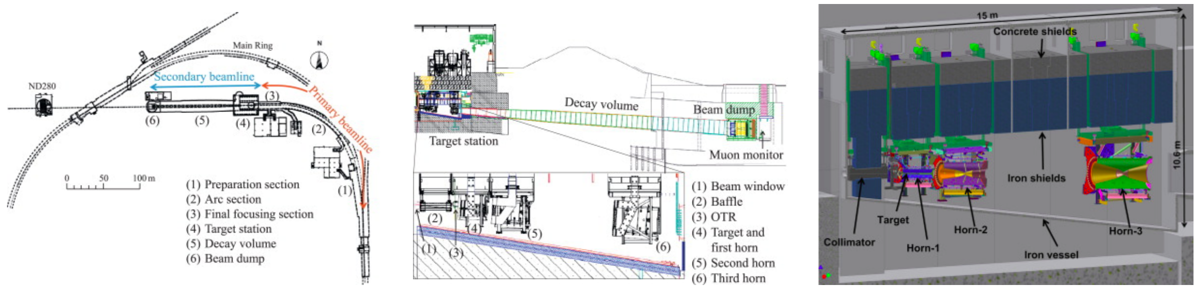

(a) Neutrino beamline **(b)** Secondary beamline **(c)** Beamline horns

Figure 1.11: The neutrino beamline at J-PARC consists of a primary and secondary beamline. (a) The primary beamline redirects the protons towards the secondary beamline [1]. (b) In the secondary beamline, the protons are impinged on a cylindrical target producing mostly pions. The pions are focused using in sequence horns and decay in a long decay volume. Any non-decayed particles are stopped at the beam dump. (c) A further zoomed in cross section of the target station showing the target and focusing horns [18].

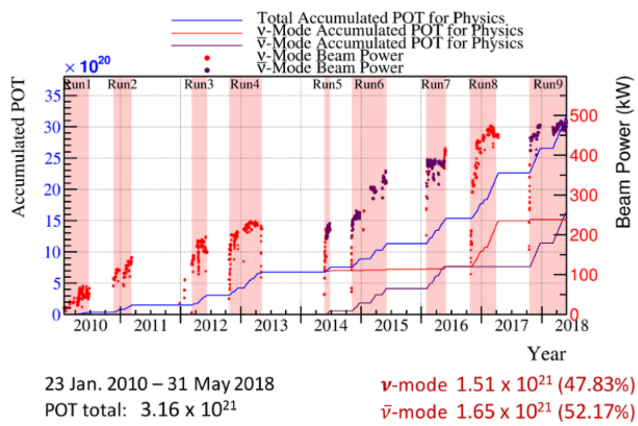

Figure 1.12: T2K accumulated protons on target since 2010 shows a steady increase in beam power over time. The gap between Run2 and Run3 is due to the damage suffered at J-PARC after the 2011 Tōhoku earthquake.

J-PARC continues to improve the MR proton delivery since T2K begin in 2010. T2K has run with both +250kA and -250kA horn currents with increasing beam power over time. Focusing positively charged pions with +250kA horn current is called forward horn current (FHC) mode or ν-mode. Similarly, using -250kA horn current is called reverse horn current (RHC) or $\bar{\nu}$-mode. The aggregate running periods for T2K for both FHC and RHC are shown in Figure 1.12 on page 27 in units of protons on target (POT or PoT).

1.2.2 T2K Near Detectors

1.2.3 Far Detector: Super-Kamiokande

1.2.4 Oscillation Analysis

The number of reconstructed neutrino events of flavor α observed at the far detector (FD) is sum of all true charged current (CC) events $S^{\mathrm{FD}}_{\nu_\alpha}$ and backgrounds B

$$N^{\mathrm{FD}}_{\nu_\alpha} = S^{\mathrm{FD}}_{\nu_\alpha} + B$$

where

$$\begin{aligned} S^{\mathrm{FD}}_{\nu_\alpha} \to S^{\mathrm{FD}}_{\nu_\alpha}\left(p_\alpha, \theta_\alpha; \vec{o}\right) = \sum_i \sum_\beta \mathcal{P}_{\nu_\beta \to \nu_\alpha}\left(E_{\nu,i}; \vec{o}\right) \times \sigma^{\mathrm{CC}}_{\nu_\alpha}\left(E_{\nu,i}\right) \\ \times \Phi^{\mathrm{FD}}_{\nu_\alpha}\left(E_{\nu,i}\right) \times T^{\mathrm{FD}} \times \epsilon^{\mathrm{FD}}\left(p_\alpha, \theta_\alpha\right) \end{aligned}$$

where

$$\sigma^{\mathrm{CC}}_{\nu_\alpha}\left(E_\nu\right) = \sum_{\mathrm{mode}} \left[\sigma\left(E_\nu\right)\right]_{\nu_\alpha \mathrm{CC\ mode}}$$

Bibliography

[1] K. Abe et al. The T2K Experiment. *Nucl. Instrum. Meth.*, A659:106–135, 2011. 22, 25, 27

[2] K. Abe et al. Observation of Electron Neutrino Appearance in a Muon Neutrino Beam. *Phys. Rev. Lett.*, 112:061802, 2014. 23

[3] K. Abe et al. Search for CP Violation in Neutrino and Antineutrino Oscillations by the T2K Experiment with 2.2×10^{21} Protons on Target. *Phys. Rev. Lett.*, 121:171802, Oct 2018. 23

[4] C. Adams et al. The Long-Baseline Neutrino Experiment: Exploring Fundamental Symmetries of the Universe. 2013. arXiv:1307.7335. 4, 20, 22

[5] Jiro Arafune, Masafumi Koike, and Joe Sato. CP violation and matter effect in long baseline neutrino oscillation experiments. *Phys. Rev. D*, 56:3093–3099, Sep 1997. 21

[6] J-PARC Center. What is J-PARC?, January 2019. https://j-parc.jp/researcher/en/about/what/index.html, Accessed on 26 January 2019. 24

[7] A. de Gouvea et al. Working Group Report: Neutrinos. In *Proceedings, 2013 Community Summer Study on the Future of U.S. Particle Physics: Snowmass on the Mississippi*, 2013. arXiv:1310.4340. 20

[8] I. Esteban et al. Global analysis of three-flavour neutrino oscillations: synergies and tensions in the determination of $\theta_{23}, \delta_{\mathrm{CP}}$, and the mass ordering. 2018. arXiv:1811.05487. 21

[9] A. Ferrero. The ND280 Near Detector of the T2K Experiment. *AIP Conference Proceedings*, 1189(1):77–82, 2009. 23

[10] S. Fukuda et al. The Super-Kamiokande detector. *Nuclear Instruments and Methods in Physics Research Section A: Accelerators, Spectrometers, Detectors and Associated Equipment*, 501(2):418 – 462, 2003. 23

[11] Susumu Igarashi. Recent Progress of J-PARC MR Beam Commissioning and Operation. In *Proceedings, 57th ICFA Advanced Beam Dynamics Workshop on High-Intensity and High-Brightness Hadron Beams (HB2016): Malmö, Sweden, July 3-8, 2016*, page MOAM6P60, 2016. 26

[12] C. Jarlskog. A Basis Independent Formulation of the Connection Between Quark Mass Matrices, CP Violation and Experiment,. *Z. Phys.*, C29:491–497, 1985. 19

[13] Z Maki, M. Nakagawa, and S. Sakata. Remarks on the Unified Model of Elementary Particles. *Progr. Theor. Exp. Phys.*, 28(5), 1962. 16

[14] B. Pontecorvo. Inverse Beta Processes and Nonconservation of Lepton Charge. *J. Exp. Theor. Phys.*, 28(5), 1957. 16

[15] P. K. Saha et al. Simulation, measurement, and mitigation of beam instability caused by the kicker impedance in the 3-GeV rapid cycling synchrotron at the Japan Proton Accelerator Research Complex. *Phys. Rev. Accel. Beams*, 21:024203, Feb 2018. 26

[16] Andrei D Sakharov. Violation of CP invariance, C asymmetry, and baryon asymmetry of the universe. *Soviet Physics Uspekhi*, 34(5):392, 1991. 22

[17] N. Schmitz. *Neutrinophysik*. Teubner, Stuttgart, 1997. 16

[18] T. Sekiguchi et al. Development and operational experience of magnetic horn system for T2K experiment. *Nuclear Instruments and Methods in Physics Research Section A: Accelerators, Spectrometers, Detectors and Associated Equipment*, 789:57 – 80, 2015. 27

[19] M. Tanabashi et al. The Review of Particle Physics. *Phys. Rev. D*, 98(030001), 2018. 17, 21

[20] Y. Yamazaki, editor. *Accelerator technical design report for high-intensity proton accelerator facility project, J-PARC*. Number 2002-013. Japan Atomic Energy Research Institute, 2003. 26

[21] Kai Zuber. *Neutrino Physics*. CRC Press, Boca Raton, FL., 2nd edition, 2012. 2, 11, 16